

## Isotropic Knight shift of metallic carbon nanotubes

Oleg V. Yazyev\* and Lothar Helm

*Ecole Polytechnique Fédérale de Lausanne (EPFL), Institute of Chemical Sciences and Engineering, CH-1015 Lausanne, Switzerland*

(Received 31 August 2005; revised manuscript received 3 October 2005; published 15 December 2005)

We study the isotropic  $^{13}\text{C}$  Knight shifts of conducting carbon nanotubes from first principles. We find that the values of the shifts provide information about the chirality indices of nanotubes. For carbon nanotubes wider than 0.5 nm the dominating spin-polarization effect leads to a small (several ppm) negative isotropic Knight shift. The shift is inversely proportional to the diameter for conducting nanotubes wider than 1.5 nm. Larger positive Knight shifts (hundreds of ppm) are predicted for ultranarrow zigzag nanotubes because of the bands with a significant degree of rehybridization crossing the Fermi level. The isotropic  $^{13}\text{C}$  and  $^{19}\text{F}$  Knight shifts of chemically modified carbon nanotubes are studied for the example of fluorinated (4,4)- $\text{C}_2\text{F}$  single-wall nanotube.

DOI: [10.1103/PhysRevB.72.245416](https://doi.org/10.1103/PhysRevB.72.245416)

PACS number(s): 81.07.De, 71.15.Dx, 71.20.Tx, 76.60.Cq

Carbon nanotubes (CNTs) have attracted enormous interest due to their unusual physical properties. For instance, CNTs may be either metallic or semiconducting with the electronic properties depending on their atomic structure.<sup>1</sup> This promises many applications of CNTs in technology. Particularly, different varieties of metallic CNTs may be used as the components of future nanometer-sized electronic devices, electrochemical devices, and conducting composites.<sup>2</sup> Nowadays, CNTs are routinely produced in large quantities. Efficient methods for separation of metallic and semiconducting CNTs and their further purification have been developed.<sup>3</sup> At this stage, the nuclear magnetic resonance (NMR) technique widely used in chemistry can be applied to the study of the composition of CNT samples. Significant progress has recently been achieved in experimental NMR of carbon nanotubes. The  $^{13}\text{C}$  nuclear spins of semiconducting and metallic CNTs have been identified by means of spin-lattice relaxation rate measurements,<sup>4</sup> and the NMR spectra of single-wall CNTs, purified from paramagnetic impurities, have been obtained.<sup>5</sup> In the latter case, the NMR signal has been resolved into the contributions of semiconducting and metallic CNTs at a ppm-level resolution.

The shift of the Larmor frequency of the nuclear spin is described by the chemical shift tensor,  $\vec{\delta} = \vec{\sigma}_{ref} - \vec{\sigma} + \vec{K}$ , which is defined by the magnetic shielding relative to a standard reference,  $\vec{\sigma}_{ref} - \vec{\sigma}$ , and the Knight shift tensor  $\vec{K}$ , which originates from the Pauli paramagnetism, occurring only in metals.<sup>6</sup> One often splits tensorial contributions into corresponding scalar isotropic parts (e.g.,  $K_{iso} = \frac{1}{3} \text{Tr}[\vec{K}]$  for the Knight shift contribution) and remaining traceless anisotropy tensors. In reality solid samples of carbon nanotubes are orientationally disordered. The isotropic chemical shift  $\delta_{iso}$  and partial information about chemical shift anisotropy tensor can be obtained from the static NMR measurements of such samples. Moreover, high resolution solid state NMR experiments are often performed under isotropic averaging conditions such that only isotropic quantities are measured. Latil *et al.*<sup>7</sup> theoretically predicted a separation of about 11 ppm between the isotropic chemical shifts of metallic and insulating CNTs due to the London ring current contribution to the magnetic shielding. However, the ring current contribution

does not provide more details about the atomic structure of CNTs which is commonly characterized by the pair of chirality indices  $(n, m)$ .

In the present study, we investigate the isotropic Knight shifts of metallic CNTs using a theoretical approach. We show that the values of the shifts provide information about the chirality indices of conducting CNTs in a sample. For narrow CNTs isotropic Knight shifts achieve significant values. Moreover, high-resolution NMR measurements of isotropic Knight shifts can be used to study the electronic structure of chemically modified, bundled, and multiwalled CNTs. We aim to stress the value of NMR as an experimental method for the investigation of these promising materials.

The isotropic Knight shift

$$K_{iso} = \frac{8\pi}{3} (\langle |\psi(0)|^2 \rangle + \eta) \chi_p, \quad (1)$$

originates from the Fermi contact magnetic interaction between the conduction electron spin and the nuclear spin. One can separate the contributions due to the effects of (i) the conduction electrons, which is proportional to the squared magnitude of conduction band wave function at the point of the nucleus  $\psi(0)$ , and (ii) the ensemble of spin-polarized valence bands and atomic core states.<sup>8</sup> The latter term can be collected in the common parameter  $\eta$ . The Pauli spin susceptibility,  $\chi_p$ , is proportional to the density of states at the Fermi level,  $n(\epsilon_F)$ . Thus,  $K_{iso}$  provides an information about the conduction states which can be related to the atomistic structure of the metallic system under investigation.

In a single two-dimensional graphite layer, graphene,  $\psi(0) = 0$  because conduction bands have  $\pi_{\perp}$  character and all nuclei lie in the nodal plane of these states. Rolling up the graphene sheet into a carbon nanotube causes partial  $sp^2$ - $sp^3$  rehybridization which means that the  $\pi_{\perp}$  states receive  $s$  character rapidly increasing with a decreasing CNT diameter. The rehybridization contribution to the isotropic Knight shift is positive. The exchange spin-polarization effects on Knight shift are relatively well studied for the kindred class of conducting compounds, alkali metal graphite intercalates. Negative isotropic Knight shifts up to 100 ppm

in magnitude were measured experimentally<sup>9</sup> for these systems. However, the density of states at the Fermi level in graphite intercalates is higher compared to that of metallic carbon nanotubes.<sup>1</sup> This reduces the estimates of the negative spin-polarization contribution to the order of several ppm.

Other possible contributions to isotropic Knight shifts in CNTs concern ultranarrow, chemically modified, bundled, and multiwalled CNTs. (i) It has been shown by first principles calculations<sup>10</sup> that  $(n, 0)$ ,  $(n=3-6)$  single-wall CNTs (termed irregular CNTs below, regular otherwise) are true metals. The density of states at the Fermi level,  $n(\epsilon_F)$ , is higher than predicted by the zone folding approximation<sup>1</sup> and the conduction bands might have higher  $s$  character in these cases. (ii) For chemically functionalized CNTs additional possibilities can be exploited. A chemical modification may change both  $n(\epsilon_F)$  as well as the spatial character of the conduction states. In addition, introduced nuclei of functional groups may also experience isotropic Knight shifts. This suggests to perform NMR measurements on nuclei other than  $^{13}\text{C}$  in order to probe the conduction states of a sample. (iii) Nanotube bundling may affect the band structure of CNTs by breaking the metallicity of otherwise metallic CNTs or closing the gap in semiconducting ones. The pseudogap opening in conducting nanotubes has been observed experimentally and studied theoretically<sup>11</sup> while the band gap closing in otherwise semiconducting nanotubes was predicted theoretically.<sup>12</sup> Reich *et al.* showed in their computational study<sup>12</sup> that in  $(10,0)$  nanotube bundles the gap between  $\pi$  and  $\pi^*$  bands closes up due to the dispersion perpendicular to the nanotube axis. The curvature-induced metallization of double-wall semiconducting nanotubes has also been predicted recently.<sup>13</sup>

Unlike its isotropic contribution, the Knight shift anisotropy originates from the dipole-dipole interaction between the electron spin and the nuclear spin. The dipolar contribution can be accessed by analyzing the static line shape of the NMR spectrum or through the nuclear relaxation rate measurements. In the case of conducting CNTs, the dipolar Knight shift originates from the direct contribution of conduction  $\pi$  states and is almost unaffected by the spin polarization and  $sp^2$ - $sp^3$  rehybridization effects.<sup>14</sup> Its value provides direct information about  $n(\epsilon_F)$  what was used in a number of studies of carbon nanotubes and graphite intercalation compounds.<sup>4,7,15</sup>

The computational method we use is based on the all-electron density functional theory (DFT) approach within periodic boundary conditions<sup>16</sup> implemented in the GAUSSIAN 03 code.<sup>17</sup> Following the methodology of Weinert *et al.*,<sup>18</sup> we perform unrestricted self-consistent field (SCF) calculations with arbitrary external magnetic field  $H$ . In order to keep the numerical errors of the SCF calculations small it is necessary to apply strong magnetic fields, about two orders of magnitude stronger than the ones conventionally used in the NMR measurement. For instance, in the case of the  $(6,6)$  CNT calculation an external magnetic field of  $1.3 \times 10^7$  G was applied in order to achieve magnetization of 0.002 electrons per atom. The corresponding Fermi contact hyperfine field at the  $^{13}\text{C}$  nuclei is about 21 G in this calculation. We confirmed that for these systems such strong external fields are

still in the linear regime for the change of the hyperfine field with respect to the external one. The calculated isotropic Knight shift

$$K_{iso} = \frac{8\pi}{3} \gamma_e \frac{\rho^{\uparrow}(0) - \rho^{\downarrow}(0)}{H}, \quad (2)$$

with  $\gamma_e$  being the electron gyromagnetic ratio and  $\rho^{\uparrow(\downarrow)}(0)$  being the spin-up (-down) electron density at the nucleus site. The SCF approach permits us to include explicit contributions coming from the magnetization of the conduction electrons and from possible spin-polarization effects and the exchange-correlation spin susceptibility enhancement.<sup>19</sup>

The Becke exchange<sup>20</sup> and Lee-Yang-Parr correlation<sup>21</sup> generalized gradient approximation density functionals (BLYP) and Dunning's D95(d) Gaussian-type orbital basis set<sup>22</sup> have been used in our calculations. In this basis set both valence and core functions are double split as a necessary condition for an accurate description of spin polarization. We found that this basis set is a reasonable compromise between accuracy and computational cost. In order to check the accuracy of this combination of basis set and density functional we have performed test calculations of  $^{13}\text{C}$  isotropic hyperfine coupling constant for the planar  $\text{CH}_3$  radical. A number of detailed experimental works and theoretical calculations are available for this simple radical. In this system the unpaired electron resides on an orbital of pure  $p$  character. Thus, the Fermi contact contribution of the singly occupied molecular orbital to the  $^{13}\text{C}$  isotropic hyperfine coupling constant is zero like in a graphene sheet. This isotropic coupling can be reproduced with good accuracy by the DFT calculations (see, e.g., Ref. 23). At the chosen level of theory the calculated  $^{13}\text{C}$  isotropic hyperfine coupling constant of the  $\text{CH}_3$ -radical amounts to 26.40 G, while the BLYP basis set limit value is 26.13 G. The coupled-cluster singles and doubles (CCSD) theory in combination with D95(d) basis set gives 27.72 G. All these results compare well with the experimental value of 28.4 G determined by Chipman<sup>24</sup> for the planar radical. The crucial step for an accurate calculation of Knight shifts using a self-consistent approach is the Brillouin zone integration. We have used an interpolative approach, which is a one-dimensional version of the linear tetrahedron method.<sup>25</sup> No thermal smearing has been applied and possible band crossings at the Fermi level have been resolved,<sup>26</sup> if necessary. In all our calculations the uniform Brillouin zone integration mesh consists of 512  $\mathbf{k}$  points.

In this work, we study conducting armchair  $(n, n)$  ( $n=3-12$ ) and zigzag  $(n, 0)$  ( $n=3-6, 9, 12, 15$ ) nanotubes which have diameters up to 1.6 nm. The structures of these nanotubes have been generated<sup>27</sup> assuming a 1.421 Å carbon-carbon bond distance. The geometries of the ultranarrow zigzag nanotubes  $(n, 0)$  ( $n=3-6$ ) have been relaxed at the same level of theory as the one used for the calculation of Knight shifts. This is necessary since an effect of the bond length alternation<sup>28</sup> becomes important for ultranarrow CNTs. The effects of electron-phonon coupling and small curvature-induced band gap<sup>29</sup> in wider zigzag CNTs have not been taken into account.

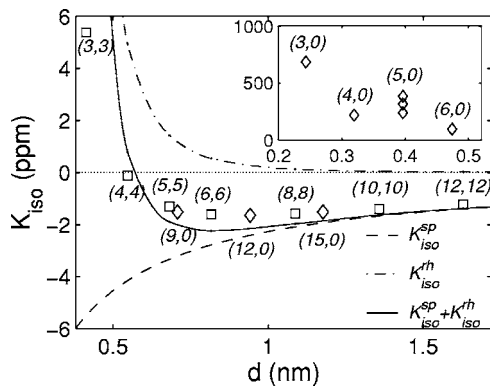


FIG. 1. Isotropic Knight shifts of conducting single-wall CNTs. In regular metallic nanotubes  $K_{iso}$  shows dependence on the nanotube diameter as a result of interplay between the spin polarization ( $K_{iso}^{sp}$ ) and the rehybridization ( $K_{iso}^{rh}$ ) contributions. The squares and diamonds indicate the calculated shifts for armchair and metallic zigzag CNTs, correspondingly. The curves show estimated shift as a function of CNT diameter and its individual contributions (see text). Isotropic Knight shifts of ultranarrow conducting CNTs are shown in the inset. Three different types of  $^{13}\text{C}$  nuclei in (5,0) CNT can be recognized.

The calculated values of  $K_{iso}$  for regular metallic CNTs are shown in Fig. 1 as a function of their diameter. The shifts have been predicted to be negative for the CNTs with diameter larger than 0.5 nm while a positive value of 5.4 ppm has been predicted for the narrow (3,3) CNT. We explain the observed trend as the sum of the contributions due to the spin polarization for the flat graphene sheet ( $K_{iso}^{sp}$ ) and due to the curvature-induced rehybridization ( $K_{iso}^{rh}$ ). The spin-polarization contribution is proportional to the density of states at the Fermi level,  $K_{iso}^{sp} = Bn(\epsilon_F)$ . The negative constant  $B$  equal to  $-228 \text{ ppm} \cdot \text{eV} \cdot \text{carbon atom} \cdot \text{spin}$  has been predicted on the basis of calculations for the flat graphene sheet. This result can be compared to the experimental range between  $-530$  and  $-270 \text{ ppm} \cdot \text{eV} \cdot \text{carbon atom} \cdot \text{spin}$  for  $\text{MC}_n$  ( $M=\text{K, Cs}; x \geq 8$ ) graphite intercalation compounds.<sup>9</sup>

The SCF spin-density induced by the external magnetic field is shown in Fig. 2. The positive spin density due to the direct magnetization of the graphene  $\pi$  and  $\pi^*$  conduction band electrons prevails. However, the negative magnetization has been observed in the graphene plane ( $z=0$ ). It achieves absolute maxima at the sites of carbon nuclei. This can be explained by both negative  $1s$  core and  $2s$  spin polarization. The rehybridization contribution is estimated as  $K_{iso}^{rh} = 8\pi/3 [m\psi_{2s}^2(0)]\chi_p$ , where  $m$  is the  $s$  content of the  $\pi$  orbital as defined in the  $\pi$ -orbital axis vector (POAV) analysis<sup>30</sup> and  $\psi_{2s}(0)$  is the magnitude of the carbon atom  $2s$  wave function at the point of the nucleus. This contribution is significant only for the narrowest CNTs and increases very fast with decreasing diameter. It is remarkable that the estimated trend in Knight shifts reproduces calculated values.

From our calculations we conclude that the isotropic Knight shift of average diameter ( $d > 0.6$  nm) metallic CNTs is on the order of 1–2 ppm towards lower frequencies. These values can be compared to the difference of about 8 ppm between the chemical shifts of semiconducting and metallic

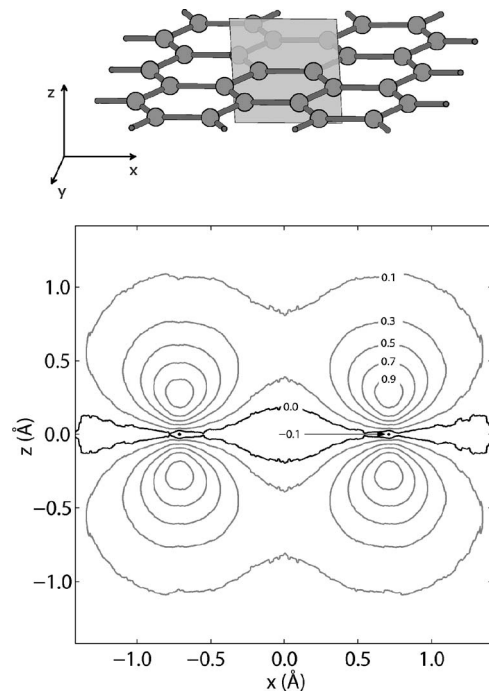


FIG. 2. Calculated SCF spin density (arb. units) for flat graphene sheet in an external magnetic field in the plane orthogonal to the graphene sheet (top). The maximum value of spin density on the contour plot (bottom) is 1.0. Position of a carbon atom and a contour line corresponding to the spin-density value of  $-0.1$  is indicated by the arrow.

single-wall CNTs obtained experimentally using solid-state NMR.<sup>5</sup> This experimental value is 3 ppm smaller than the difference of 11 ppm, theoretically predicted when taking into account only ring current effects. The calculated negative isotropic Knight shift explains the difference in predicted and experimentally observed values. Knight shifts of wider ( $d > 1.6$  nm) CNTs, which are not considered here can be obtained by means of extrapolation based only on the graphenic spin-polarization contribution. Rehybridization contribution can safely be neglected for wider CNTs. In this case, a measured Knight shift reflects the density of states at the Fermi level in a direct way.

However, ultranarrow irregular CNTs show much larger positive isotropic Knight shifts (Fig. 1, inset) as a result of significant rehybridization of the conduction band states and higher  $n(\epsilon_F)$ . The highest predicted value is +685 ppm for the (3,0) nanotube. For the (5,0) single-wall CNT, three types of nuclei can be distinguished because this CNT is predicted to be slightly flattened. Similar observations concerning the geometry of the (5,0) CNT have been made in Ref. 16.

As an example of a chemically functionalized system, the isotropic Knight shifts of the fluorinated (4,4) armchair CNT (Ref. 31) have been calculated. The stable configuration of the single-wall (4,4)- $\text{C}_2\text{F}$  CNT is taken from the computational study of Bettinger *et al.*<sup>32</sup> For the benefit of the reader, the structure of the unmodified and fluorinated (4,4) CNTs are shown in Fig. 3. In this case chemical functionalization causes complete rehybridization to  $sp^3$  state of half of the carbon atoms without breaking the metallicity. The contribu-



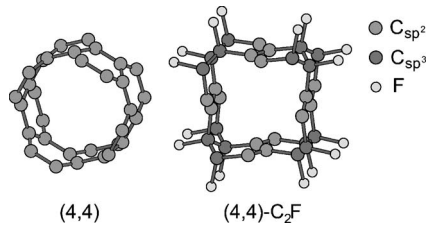


FIG. 3. Atomic structures of unmodified and fluorinated (4,4) CNTs. The hybridization states of carbon atoms are indicated. Two unit cells are shown in both cases.

tion of these atoms to the conduction states is smaller but their relative  $s$  contribution is higher. Thus, a positive Knight shift for such atoms is expected. The other atoms are arranged into flat “strips” which are responsible for conductivity. A negative graphenic shift is expected on the nuclei of  $C_{sp^2}$  atoms. Chemical modification also leads to an increase of  $n(\epsilon_F)$  in this case,  $0.063 (\text{eV} \cdot C_{sp^2} \text{ atom} \cdot \text{spin})^{-1}$  compared to  $0.020 (\text{eV} \cdot C_{sp^2} \text{ atom} \cdot \text{spin})^{-1}$  for the unmodified (4,4) CNT. Our calculations predict  $-7.5$  ppm,  $+18.6$  ppm, and  $+21.3$  ppm isotropic Knight shifts for the nuclei of  $C_{sp^2}$ ,  $C_{sp^3}$ , and F atoms, respectively. The difference in Knight shifts among the two types of carbon nuclei is 26.1 ppm. Thus the Knight shift contribution to the total chemical shift

is of similar order of magnitude with the typical difference (about 100 ppm) in orbital chemical shifts of  $C_{sp^2}$  and  $C_{sp^3}$  nuclei. In addition, the Knight shift anisotropy of  $C_{sp^3}$  and of F nuclei is smaller compared to that of  $C_{sp^2}$  nuclei that favors the observation of narrow NMR signals.

In conclusion, our results show that the isotropic Knight shifts of metallic CNTs, except ultranarrow ones, reflect the density of states at the Fermi level. High-resolution NMR can be used to study the distribution of diameters of the conducting CNTs in a sample. Ultranarrow zigzag CNTs possess large positive isotropic Knight shifts characteristic of their chirality indices. Knight shifts can serve as the unambiguous spectroscopic signatures of these unusual structures. Finally, Knight shift measurements can be useful to study chemically functionalized CNTs. The results of our theoretical study provide a perspective for studying carbon nanostructures using NMR.

The authors acknowledge A. Borel, O. A. von Lilienfeld, J. Van Der Klink, K. Kudin, A. Pasquarello, and I. Tavernelli for discussions. The authors thank S. Reich and P. Ordejón for providing data on their calculations of bundled carbon nanotubes. O.Y. thanks the Swiss National Science Foundation for financial support. The computational resources were provided by the Swiss Center for Scientific Computing.

\*Electronic address: oleg.yazyev@epfl.ch

- <sup>1</sup>J. W. Mintmire and C. T. White, Phys. Rev. Lett. **81**, 2506 (1998); J. W. Mintmire and C. T. White, Appl. Phys. A: Mater. Sci. Process. **67**, 65 (1998).
- <sup>2</sup>S. H. Baughman, A. A. Zakhidov, and W. A. de Heer, Science **297**, 787 (2002).
- <sup>3</sup>Yu. Maeda, W. Wang, S.-Y. Xie, Y. Lin, K. A. S. Fernando, X. Wang, L. Qu, B. Chen, and Y.-P. Sun, J. Am. Chem. Soc. **127**, 10287 (2005).
- <sup>4</sup>X.-P. Tang, A. Kleinhammes, H. Shimoda, L. Fleming, K. Y. Bennoune, S. Sinha, C. Bower, O. Zhou, and Y. Wu, Science **288**, 492 (2000).
- <sup>5</sup>A. Kitaygorodskiy, W. Wang, S.-Y. Xie, Y. Lin, K. A. S. Fernando, X. Wang, L. Qu, B. Chen, and Y.-P. Sun, J. Am. Chem. Soc. **127**, 7517 (2005).
- <sup>6</sup>W. D. Knight, Phys. Rev. **76**, 1259 (1949).
- <sup>7</sup>S. Latil, L. Henrard, C. Goze Bac, P. Bernier, and A. Rubio, Phys. Rev. Lett. **86**, 3160 (2001); C. Goze Bac, S. Latil, P. Laudin, V. Jourdain, J. Conard, L. Duclaux, A. Rubio, and P. Bernier, Carbon **40**, 1825 (2002).
- <sup>8</sup>V. Jaccarino and Y. Yafet, Phys. Rev. **133**, A1630 (1964); G. D. Gaspari, W.-M. Shyu, and T. P. Das, *ibid.* **134**, A852 (1964).
- <sup>9</sup>J. Conard, H. Estrade, P. Lauginie, H. Fuzellier, G. Furdin, and R. Vasse, Physica B & C **99B**, 521 (1980).
- <sup>10</sup>M. Machón, S. Reich, C. Thomsen, D. Sánchez-Portal, and P. Ordejón, Phys. Rev. B **66**, 155410 (2002); I. Cabria, J. W. Mintmire, and C. T. White, Phys. Rev. B **67**, 121406(R) (2003).
- <sup>11</sup>P. Delaney, H. J. Choi, J. Ihm, S. G. Louie, and M. L. Cohen, Phys. Rev. B **60**, 7899 (1999); M. Ouyang, J.-L. Huang, C. L. Cheung, and C. M. Lieber, Science **292**, 702 (2001).
- <sup>12</sup>S. Reich, C. Thomsen, and P. Ordejón, Phys. Rev. B **65**, 155411 (2002).
- <sup>13</sup>S. Okada and A. Oshiyama, Phys. Rev. Lett. **91**, 216801 (2003).
- <sup>14</sup>C. H. Pennington and V. A. Stenger, Rev. Mod. Phys. **68**, 855 (1996).
- <sup>15</sup>J. Conard, M. Gutierrez-le Brun, P. Lauginie, H. Estrade-Szwarcckopf, and G. Hermann, Synth. Met. **2**, 227 (1980).
- <sup>16</sup>K. N. Kudin and G. E. Scuseria, Phys. Rev. B **61**, 16440 (2000).
- <sup>17</sup>M. J. Frisch *et al.*, GAUSSIAN 03, Revision C.01, Gaussian, Inc., Wallingford, CT, 2004, <http://www.gaussian.com>
- <sup>18</sup>M. Weinert and A. J. Freeman, Phys. Rev. B **28**, 6262 (1983).
- <sup>19</sup>C. Herring, in *Magnetism*, edited by G. T. Rado and H. Suhl (Academic, New York, 1966), Vol. 4, pp. 273–297.
- <sup>20</sup>A. D. Becke, Phys. Rev. A **38**, 3098 (1988).
- <sup>21</sup>C. Lee, W. Yang, and R. G. Parr, Phys. Rev. B **37**, 785 (1988).
- <sup>22</sup>T. H. Dunning, Jr. and P. J. Hay, in *Modern Theoretical Chemistry*, edited by H. F. Schaefer III (Plenum, New York, 1976), Vol. 3, pp. 1–28.
- <sup>23</sup>O. V. Yazyev, I. Tavernelli, L. Helm, and U. Röthlisberger, Phys. Rev. B **71**, 115110 (2005).
- <sup>24</sup>D. M. Chipman, Theor. Chim. Acta **82**, 93 (1992).
- <sup>25</sup>O. Jepsen and O. K. Andersen, Solid State Commun. **9**, 1763 (1971); P. E. Blöchl, O. Jepsen, and O. K. Andersen, Phys. Rev. B **49**, 16223 (1994); O. V. Yazyev, E. N. Brothers, K. N. Kudin, and G. E. Scuseria, J. Chem. Phys. **121**, 2466 (2004).
- <sup>26</sup>O. V. Yazyev, K. N. Kudin, and G. E. Scuseria, Phys. Rev. B **65**, 205117 (2002).
- <sup>27</sup>J. T. Frey and D. J. Doren, TUBEGEN 3.1, University of Delaware, Newark, DE, 2003.
- <sup>28</sup>O. Gülseren, T. Yildirim, and S. Ciraci, Phys. Rev. B **65**, 153405 (2002).

- (2002).
- <sup>29</sup>C. L. Kane and E. J. Mele, Phys. Rev. Lett. **78**, 1932 (1997).
- <sup>30</sup>R. C. Haddon, J. Am. Chem. Soc. **108**, 2837 (1986).
- <sup>31</sup>E. T. Mickelson, C. B. Huffman, A. G. Rinzler, R. E. Smalley, R. H. Hauge, and J. L. Margrave, Chem. Phys. Lett. **296**, 188 (1998).
- <sup>32</sup>H. F. Bettinger, K. N. Kudin, and G. E. Scuseria, J. Am. Chem. Soc. **123**, 12849 (2001).